

# Diffractive Dissociation into $\pi^- \pi^- \pi^+$ Final States at COMPASS

Florian Haas for the COMPASS collaboration

*Physik Department E18, Technische Universität München  
James Franck Str., D-85748 Garching*

**Abstract.** QCD predicts gluonic excitations like hybrids to contribute to the meson spectrum in addition to  $q\bar{q}$  pair configurations. The most promising way to identify such states is the search for  $J^{PC}$  quantum number combinations which are forbidden in the constituent quark model. The fixed target COMPASS experiment at CERN offers the opportunity to search for such states in the light quark sector with an unprecedented statistics.

Diffractive reactions of 190 GeV/c pions on a lead target were studied by COMPASS during a pilot run in 2004. A Partial Wave Analysis (PWA) of the  $\pi^- \pi^- \pi^+$  final state with 42 waves including acceptance corrections through a phase-space Monte Carlo simulation of the spectrometer was performed. The exotic  $\pi_1(1600)$  meson with quantum numbers  $J^{PC} = 1^{-+}$  has been clearly established in the rho-pi decay channel with a mass of  $1660 \pm 10(\text{stat}) \text{ MeV}/c^2$  and a width of  $269 \pm 21(\text{stat}) \text{ MeV}/c^2$ . The improved detector performance in 2008 allows us to study this channel with significantly higher statistics. First results of the ongoing analysis of the 2008 data taking period, using a 190 GeV/c pion beam on a liquid hydrogen target are presented in this paper.

**Keywords:** hadron spectroscopy, light meson spectrum, diffraction, gluonic excitations, exotic mesons, hybrids

**PACS:** 13.25.-k, 13.85.-t, 14.40.Be, 29.30.-h

## INTRODUCTION

A meson is described by a set of quantum numbers, which are isospin  $I$  and  $G$ -parity and the total spin  $J$  with parity  $P$  and charge conjugation parity  $C$ . In the quark model mesons can be described as bound states of quarks and anti-quarks. Quantum Chromo Dynamics (QCD) predicts the existence of states which are not foreseen within the quark model. Possible states are hybrids, i.e. a system consisting of a color octet  $q\bar{q}$  pair neutralized in color by a gluonic excitation, or glueballs, consisting only of glue. The experimental identification of such states, however, is difficult due to mixing with  $q\bar{q}$  configurations with the same quantum numbers. The observation of exotic states, however, with quantum numbers not allowed in the simple quark model, e.g.  $J^{PC} = 0^{-+}, 0^{+-}, 1^{-+}, \dots$ , would give clear evidence that quark-gluon configurations beyond the quark model, as allowed by QCD, are realized in nature.

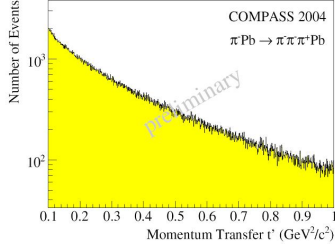
The lowest-lying hybrid is expected [1] to have exotic quantum numbers  $J^{PC} = 1^{-+}$ , and thus will not mix with ordinary mesons. Its mass is predicted in the region 1.3-2.2 GeV/c<sup>2</sup>. There are three experimental candidates for a light  $1^{-+}$  hybrid. The  $\pi_1(1400)$  was observed by E852 [2], VES [3], and Crystal Barrel [4, 5]. Another  $1^{-+}$  state, the  $\pi_1(1600)$ , decaying into  $\rho\pi$  [6, 7, 8],  $\eta'\pi$  [9, 10],  $f_1(1285)\pi$  [11, 12] and  $b_1(1235)\pi$  [12, 13] was observed in peripheral  $\pi^- p$  interactions in E852 and VES. The resonant nature of both states, however, is still heavily disputed in the community [3, 12, 14]. A third exotic state,  $\pi_1(2000)$ , decaying to  $f_1\pi$  and  $b_1\pi$  was seen in only one experiment [11, 13]. Owing to its high statistics the COMPASS experiment can contribute significantly in the light meson sector to the search for exotic mesons and glueballs.

## THE COMPASS EXPERIMENT

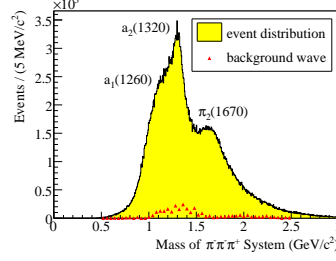
The **COM**mon **MU**on and **PRO**ton **APP**aratus for **STR**ucture and **SPE**ctroscopy [15] is located at the CERN SPS accelerator. It is a two stage magnetic spectrometer which provides a large angular acceptance over a wide momentum range. Besides calorimetry and particle identification COMPASS is equipped with a very precise charged particle tracking system. For the beam tracking, Silicon detectors around the target and Scintillating Fibres and PixelGEMs are used. Close to the beam large-size GEM detectors and Micromegas are the backbone of the tracking system. The periphery is covered by Drift Chambers and MWPCs.

## DIFFRACTIVE REACTIONS INTO 3 CHARGED PIONS ON PB IN 2004

The first years of COMPASS data taking, between 2002 and 2007, were dedicated to spin physics. In 2004 there was a short pilot run for the hadron physics program using a 190 GeV/c negative charged pion beam and a 3 mm lead target. During this short period a data sample with statistics, comparable to previous experiments, could be collected.



(a) Squared four-momentum transfer  $t'$  for diffraction of beam pions on single nucleons within the lead target, logarithmic scale.



(b) Invariant mass of the high  $t'$  data sample.

Diffraction dissociation is a process where an incoming beam particle impinges on a target and is excited to a resonance X which finally decays into a final state of particles. Here we focus on the  $\pi^- \pi^- \pi^+$  final state. The target particle stays intact, taking away the recoil momentum. In several days of data taking during the pilot run about  $4 \cdot 10^6$  diffractive events were recorded. Fig. 1a shows the distribution of the kinematic variable  $t'$  which is given by  $|t| - |t|_{min}$  where  $t$  is the square of the four-momentum transfer to the nucleus and  $|t|_{min}$  the minimum value of  $|t|$  allowed by kinematics for a given mass  $m_X$ . This analysis focuses on events in the “high  $t'$ ” region between

$0.1 \text{ GeV}^2/c^2$  and  $1.0 \text{ GeV}^2/c^2$  (see Fig. 1a) where E852 [8] observed production of the exotic  $\pi_1(1600)$  with  $J^{PC} = 1^{-+}$ . After this selection still  $4.2 \cdot 10^5$  events remain. Fig. 1b shows the  $3\pi$  invariant mass spectrum of this data sample and the intensity of the background wave with a flat distribution in 3-body phase space (triangles), obtained from a partial wave analysis, which will be described in the next section.

### 1: Kinematic Distributions.

## Isobar Model and Partial Wave Technique

The present analysis is based on the isobar model, assuming the resonance X to decay first into an intermediate isobar and a bachelor pion, with the relative orbital angular momentum  $L$  between the two. The isobar subsequently decays into a  $\pi^- \pi^+$  pair. A Partial Wave Analysis (PWA), performed in two steps, was applied to the 2004 data sample. In the first step, the mass-independent PWA, the data is divided into 40 MeV/c<sup>2</sup> wide bins in the  $3\pi$  invariant mass  $m$ , and the cross section decomposed into:

$$\sigma_{\text{indep}}(\tau, m, t') = \sum_{\epsilon=\pm 1} \sum_{r=1}^{N_r} \left| \sum_i T_{ir}^\epsilon f_i^\epsilon(t') \psi_i^\epsilon(\tau, m) / \sqrt{\int |\psi_i^\epsilon(\tau', m)|^2 d\tau'} \right|^2 \quad (1)$$

The production amplitudes  $T_{ir}^\epsilon$  are the fitting parameters. They are obtained by a maximum likelihood fit. The real functions  $f_i^\epsilon(t')$  describes the  $t'$  dependence of the cross-section while  $\tau$  represents the 5 phase-space variables of the 3-body decay. The decay amplitudes  $\psi_i^\epsilon(\tau', m)$ , where the indices  $i$  and  $\epsilon$  denote different partial waves, are characterized by a set of quantum numbers  $J^{PC} M^\epsilon [\text{isobar}] L$ .  $M$  is the absolute value of the spin projection onto the beam direction;  $\epsilon$  is the reflectivity [17], which describes the symmetry under a reflection through the production plane. The  $\psi_i^\epsilon(\tau, m)$  are described by Zemach tensors or D functions. In this analysis 41 partial waves were used. In addition an isotropic background wave was implemented.

In a second step a mass-dependent  $\chi^2$  fit is performed, parameterized by Breit-Wigner functions for the resonant part and a non-resonant background. In practice only a subset of waves is fitted. In this analysis the focus was on 6 waves, covering all important and clearly identified resonances and the exotic wave  $1^{-+} 1^+ \rho \pi P$ .

## Fit Results

Figures 2(a)-(c) shows the intensity of the three most prominent waves  $1^{++}0^+\rho\pi S$ ,  $2^{++}1^+\rho\pi D$ , and  $2^{-+}0^+f_2\pi S$ , described by Breit-Wigner functions and a coherent background, if necessary. Of peculiar interest are the fit results for the spin-exotic wave. The  $1^{-+}1^+\rho\pi P$  intensity (Fig. 3a) has the shape of a broad bump, centered at  $1.7\text{ GeV}/c^2$ , with a visible low-mass shoulder. One constant-width Breit-Wigner function (blue curve) and a non-resonant background (purple curve), possibly caused by a Deck-like effect, have been used to describe this wave. To clarify a possible resonant nature of this exotic amplitude, its interferences with well established states have been studied. Fig. 3b shows the phase difference to the  $1^{++}0^+\rho\pi S$  wave (Fig. 2a), which clearly rises between  $1.5\text{ GeV}/c^2$  and  $1.9\text{ GeV}/c^2$ . However, Fig. 3c, showing the phase difference to the  $2^{-+}0^+f_2\pi S$  wave, exhibits a rather flat phase difference, which can be explained by the presence of two resonances,  $\pi_1(1600)$  and  $\pi_2(1670)$  with similar masses and widths. An overview of the fit results of all 6 partial waves used for the mass-dependent PWA and further details can be found in [16, 18].

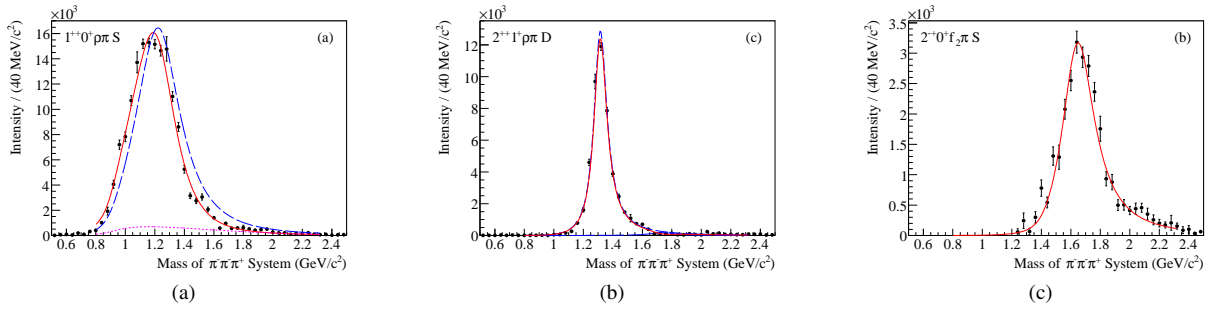


**FIGURE 2.** Intensities of major waves,  $1^{++}0^+\rho\pi S$  (a),  $2^{++}1^+\rho\pi D$  (b), and  $2^{-+}0^+f_2\pi S$  (c), the red curve is the mass dependent fit.

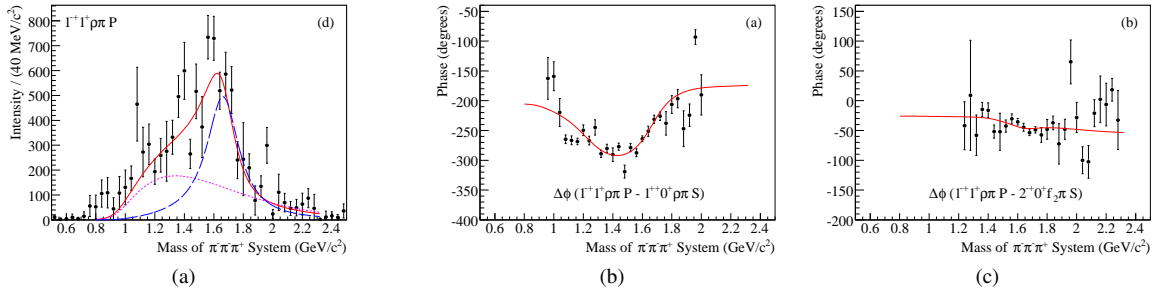


**FIGURE 3.** Intensity of the exotic wave  $1^{-+}1^+\rho\pi P$  (a), and phase differences of this wave to the  $1^{++}0^+\rho\pi S$  (b), and the  $2^{-+}0^+f_2\pi S$  (c) waves.

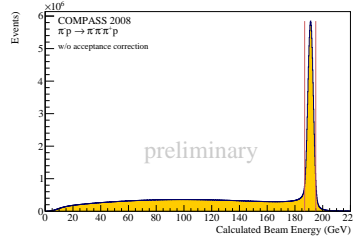
## SPECTROMETER UPGRADE

The 2008 and 2009 COMPASS data taking was mainly dedicated to meson spectroscopy. For that purpose the spectrometer was upgraded, also based on the experiences from the 2004 pilot run.

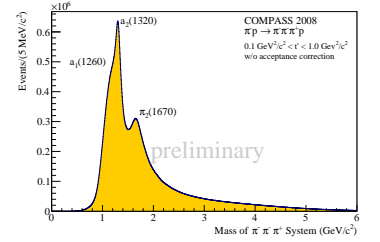
The negative hadron beam of COMPASS consists of 97% pions, 2.5% kaons and 0.5% anti-protons. In order to distinguish these incoming particle species, two CEDAR detectors, using the Cherenkov effect, were installed upstream of the target. Instead of the lead target, used in 2004, a completely new 40 cm long liquid hydrogen target was installed. Surrounding the target a new Recoil Proton Detector (RPD) was set up, triggering on recoil protons leaving the target. The RPD is one of the main components of the trigger system. Downstream of the target additional silicon microstrip detectors were placed, in order to have a good vertex resolution. Scintillating fibre detectors, used for beam tracking during the previous runs, were replaced by new PixelGEM detectors. These detectors are also able to track beam particles and particles in the vicinity of the beam, but they consist of less material. Also both electromagnetic calorimeters were upgraded with additional lead glass blocks and sampling ADCs.

## DIFFRACTIVE REACTIONS INTO 3 CHARGED PIONS ON LH<sub>2</sub> IN 2008

In 2008 a negatively charged pion beam of 190 GeV/c momentum, the same as in 2004, impinged on the hydrogen target. Since the RPD was not yet implemented in the analysis the calculated beam energy  $E_a$ , as described in [16], was used to select exclusive events. Based on this calculation only events with  $E_a$  within  $\pm 4\text{GeV}/c^2$  were accepted (Fig. 4a). As in 2004 a cut on  $t'$  between  $0.1\text{ GeV}^2/c^2$  and  $1.0\text{ GeV}^2/c^2$  was applied. Fig. 4b shows the  $3\pi$  invariant mass spectrum. During the whole 2008 campaign  $96 \cdot 10^6$  exclusive diffractive events were collected. The next section shows first fit results of a PWA applied on a subsample of these events.



(a) Calculated beam energy, red lines correspond to the exclusivity cut.

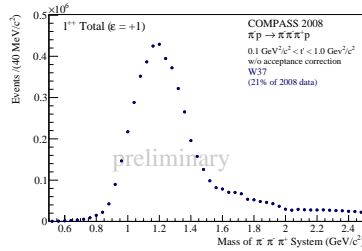


(b) Invariant mass spectrum of the  $3\pi$  system.

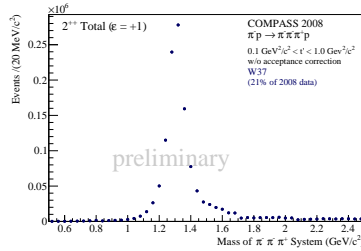
### 4: Kinematic Distributions.

### Preliminary Fit Results

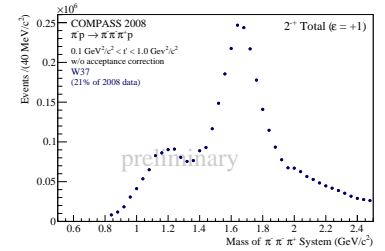
A mass-independent PWA has been carried out in  $40\text{ MeV}/c^2$  wide mass bins in a region from  $0.5 - 2.5\text{GeV}/c^2$ . This analysis is based on the same physical assumptions, including the same wave set, and the same PWA algorithm as used for the 2004 analysis. The intensities of the three major  $J^{PC}$  states,  $1^{++}$ ,  $2^{++}$ , and  $2^{-+}$ , are shown in Figures 5(a)-(c). At the present status of the analysis no acceptance correction was applied.



(a)



(b)



(c)

FIGURE 5. Total intensities for  $J^{PC} = 1^{++}$  (a),  $2^{++}$  (b), and  $2^{-+}$  (c).

A striking first (preliminary) finding concerns the  $M$ -dependence of produced waves for the different target materials. The main difference between 2004 and 2008 data samples is the target material. While in 2004 two solid lead disks were used a liquid hydrogen target with nearly the same interaction length was installed in 2008. In order to get comparable results the fit of 2004 [18] is also not acceptance corrected. Due to different amounts of statistics (2004:  $\approx 4 \cdot 10^5$  events, 2008/W37:  $\approx 1.4 \cdot 10^7$  events) both data samples are normalized to the integral of the narrow  $a_2(1320)$  resonance in the region between  $1.1\text{ GeV}/c^2$  and  $1.6\text{ GeV}/c^2$ . A clear difference in population of  $M$  substates can be seen in comparison of the two data samples. As an example the total intensities for  $J^{PC} = 1^{++}$  with different  $M$  projections are shown in Figures 6 and 7. The population of  $M = 1$  seems to be significantly higher for the heavy nuclear target (Fig. 6b) than for hydrogen (Fig. 7b). At the same time, the population of  $M = 0$  is reduced for lead (Fig. 6a) as compared to hydrogen (Fig. 7a). The total intensity for both projections, however, is rather similar (Fig. 6c and Fig. 7c).

Further studies were done in 2009 with the same spectrometer layout like in 2008 but with different targets. Data were taken with a new lead target composed of thin lead foils as well as with the Primakoff target consisting of Nickel and Tungsten. The analysis of these data could help to clarify the processes leading to this surprising  $M$ -dependence.

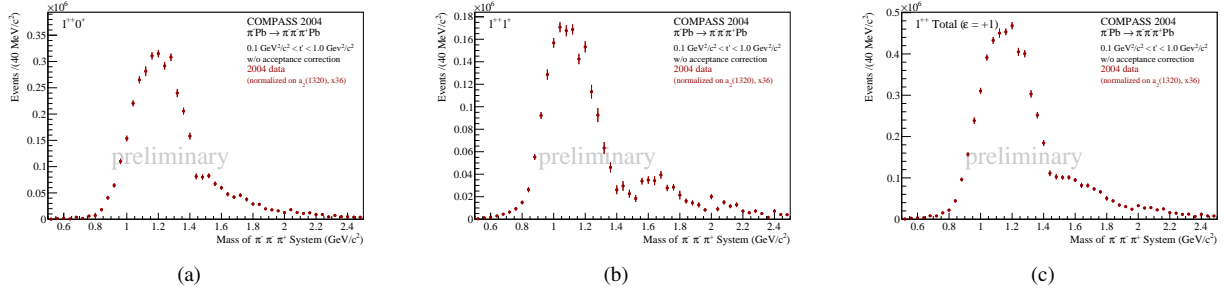


FIGURE 6. Total intensity for  $J^{PC} = 1^{++}$  with  $M = 0$  (a),  $M = 1$  (b), and for both  $M$  projections (c), for the lead target.

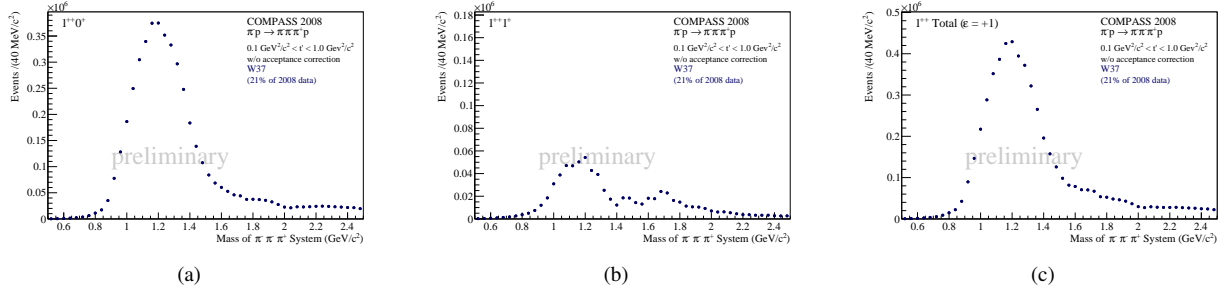


FIGURE 7. Total intensity for  $J^{PC} = 1^{++}$  with  $M = 0$  (a),  $M = 1$  (b), and for both  $M$  projections (c), for the liquid hydrogen target, the same scale is used as in Fig. 6.

## CONCLUSIONS

The COMPASS spectrometer is a powerful tool to investigate the light meson spectrum. Within a few days of data taking during a pilot run in 2004 enough statistics could be collected to perform a partial wave analysis of  $\pi^-\pi^+\pi^-$  final states. A strong signal of the spin-exotic  $\pi_1(1600)$  was observed in the  $1^{-+}1^{++}\rho\pi\text{P}$  wave. A mass-dependent fit results in a mass of  $1660 \pm 10(\text{stat}) \text{ MeV}/c^2$  and a width of  $269 \pm 21(\text{stat}) \text{ MeV}/c^2$ .

Two years of data taking, 2008 and 2009, dedicated to meson spectroscopy will improve the world statistics on diffractive by a factor of 10. First results of diffractive dissociation on hydrogen into  $\pi^-\pi^+\pi^-$  final states were shown. A striking, but yet unexplained, dependence of the production strength for different  $M$  substates of the major waves on the target material was observed.

## ACKNOWLEDGMENTS

This work is supported by the the German Bundesministerium für Bildung und Forschung, the Maier-Leibnitz-Labor der LMU und TU München, and the DFG cluster of excellence *Origin and Structure of the Universe*.

## REFERENCES

1. K. J. Juge, J. Kuti and C. Morningstar, AIP Conf. Proc. **688**, 193 (2004)
2. D. R. Thompson *et al.*, Phys. Rev. Lett. **79**, 1630 (1997)
3. V. Dorofeev *et al.*, AIP Conf. Proc. **619**, 143 (2002)
4. A. Abele *et al.*, Phys. Lett. **B423**, 175 (1998)
5. A. Abele *et al.*, Phys. Lett. **B446**, 349 (1999)
6. G. S. Adams *et al.*, Phys. Rev. Lett. **81**, 5760 (1998)
7. S. U. Chung *et al.*, Phys. Rev. **D65**, 072001 (2002)
8. Y. Khokhlov, Nucl. Phys. **A663**, 596 (2000)
9. G. M. Beladidze *et al.*, Phys. Lett. **B313**, 276 (1993)
10. E. I. Ivanov *et al.*, Phys. Rev. Lett. **86**, 3977 (2001)
11. J. Kuhn *et al.*, Phys. Lett. **B595**, 109 (2004)
12. D. V. Amelin *et al.*, Phys. Atom. Nucl. **68**, 359 (2005)
13. M. Lu *et al.*, Phys. Rev. Lett. **94**, 032002 (2005)
14. A. R. Dzerbia *et al.*, Phys. Rev. **D73**, 072001 (2006)
15. P. Abbon *et al.*, Nucl. Instr. Meth. A **577**, 455 (2007)
16. A. Alekseev *et al.*, COMPASS Collaboration, Phys. Rev. Lett. **104**, 241803 (2010)
17. S. U. Chung and T. L. Trueman, Phys. Rev. **D11**, 633 (1975)
18. Q. Weitzel, Dissertation Technische Universität München, <http://nbn-resolving.de/urn/resolver.pl?urn:nbn:de:bvb:91-diss-20080801-668430-1-0> (2008)